

Exciton binding energies in polar quantum wells with finite potential barriers

Ruisheng Zheng

*Department of Advanced Materials Science and Engineering, Faculty of Engineering, Yamaguchi University, Ube 755, Japan
and Physics Department, Inner Mongolia University, Hohhot 010021, China*

Mitsuru Matsuura

*Department of Advanced Materials Science and Engineering, Faculty of Engineering, Yamaguchi University, Ube 755, Japan
(Received 3 February 1998; revised manuscript received 26 May 1998)*

A theoretical method for studying the properties of $1s$ and $2s$ excitons in polar quantum wells with finite potential barriers is presented. Exciton-optical-phonon interaction together with an image-charge effect and discontinuity of the band masses are included in the theory. Exciton binding energies and exciton-LO-phonon interaction energies of GaAs/Ga_{1-x}Al_xAs and Zn_{1-x}Cd_xSe/ZnSe quantum wells are calculated numerically. Our theory gives correct results throughout the entire well-width range of the finite-barrier quantum wells. The properties of the $1s$ and $2s$ excitons are found very different in quantum wells. The theoretical results of the energy difference between $1s$ and $2s$ exciton states of heavy-hole excitons in these quantum-well structures are compared with the experimental data directly. The property of the excitons in polar quantum wells are discussed in the present paper. [S0163-1829(98)03640-6]

I. INTRODUCTION

Exciton binding energy is a very important parameter determining optical and electronic properties of the man-made layer materials. Exciton stability depends on the ratio of exciton binding energy to longitudinal-optical (LO) phonon energy $\hbar\omega_{LO}$, and on actual strength of the exciton-phonon coupling. Since exciton binding energies are greatly enhanced in quantum wells (QW's) by quantum confinement effect, exciton states in QW's are more stable and even exist at room temperature. In recent years, the exciton is considered a potential candidate for laser mechanisms, and have been extensively investigated experimentally and theoretically. Following the early theoretical works of Miller *et al.*,¹ Bastard *et al.*,² and Matsuura and Shinozuka,³ where the simplest model calculations for an exciton in a QW were shown, many authors calculated exciton binding energies in finite QW's.⁴⁻¹¹ In these works some detailed phenomena such as effective band mass and dielectric-constant mismatch between the well and the barrier materials, valence-band coupling, nonparabolicity of the dispersion relations, subband interference, and so on, were taken into considerations. Also, recently some authors presented improved theoretical investigations by including image charge effect.¹²⁻¹⁴ It is found that the exciton binding energy in a dielectric QW is significantly enhanced by the image charge effect even at a well width much larger than the exciton Bohr radius.

Exciton-phonon interactions in quantum wells were also studied by many authors. Chun, Won, and Pei¹⁵ studied LO phonon effect on exciton binding energy in GaAs/Ga_{1-x}Al_xAs. By using a perturbation variational technique, they investigated the dependence of ground-state binding energy on the well width and found that the correction due to the polaron effect is quite significant. With a different exciton-phonon interaction Hamiltonian, Moukhless, Fliyou, and Sayouri¹⁶ studied the same problem by employing a variational method. Both Refs. 15 and 16 used

separable trial exciton wave functions for the relative coordinate-dependent part in their calculations. It should be pointed out that the separable wave function is able to yield reasonable results for a thin QW with infinite-high barriers, but is not a reasonable candidate of the exciton wave function in a finite QW. The reason is simply that the exciton wave function penetrates extensively into barrier area in a thin-well limit. According to recent investigations,^{17,18} it is also realized that the phonon models and the exciton-phonon interaction Hamiltonian in Refs. 15 and 16 are not entirely correct pictures. Xie and Chen¹⁹ studied the ground state of both heavy- and light-hole exciton in a GaAs/Ga_{1-x}Al_xAs QW by taking all the phonon modes into account. Unfortunately, their theoretical results had been found not entirely correct.

From previous theoretical works we expect that the following effects have obvious effects on an exciton state in a polar quantum well. (1) The finite barrier-potential effect due to the discontinuity of conduction- and valence-band edges is in a dominant role in the cases of shallow or narrow QW's. (2) The exciton-optical-phonon interaction plays a very important role in exciton states since most practical QW's are composed of polar compounds. (3) The image charge effect due to the discontinuity of dielectric constants across the interface greatly affects the exciton binding energy. A synthetic investigation of these effects on the excitons in QW's is important to understand the optical and electronic properties of QW's, also in view of their application to photoelectronic devices. To our knowledge, up to now, such an investigation has not been published.

There is a practical problem of comparing theory with experiment for exciton binding energy in QW's. The published experimental results of exciton binding energies in III-V (Refs. 1, 20, and 21) and II-VI (Refs. 22-24) polar semiconductor QW's are sometimes very different from each other. The reason may be the difficulty of determining the onset of the continuum states accurately. The most reliable

measurements come from low-temperature photoluminescence or magnetoabsorption experiments on high-quality QW samples, where two clearly resolved peaks are identified as $1s$ and $2s$ exciton states. These measurements give directly the values of $|E_{2s} - E_{1s}|$. Since the ratio of E_{1s}/E_{2s} in a QW is neither four nor another constant, it is important practically to study the $2s$ exciton state in QW's and calculate the energy difference $|E_{2s} - E_{1s}|$ theoretically. It seems a better way to compare directly the exciton binding-energy difference $|E_{2s} - E_{1s}|$ with a corresponding reliable theory, and then based on the theory to determine the exciton binding energy of the ground state more accurately.

Very recently, we presented a theoretical method for investigating the properties of exciton-optical-phonon interaction systems in polar semiconductor QW's (Refs. 25 and 26) in detail. The subband effect, the image charge effect, and the anisotropy mass effect are incorporated in the theory. By using an improved variational method and nonseparable trial exciton wave functions for the relative coordinate-dependent part, we obtained expressions of bound-state energy and an average virtual phonon number of an exciton-phonon interaction system in an infinite polar QW. It was shown that our theory is valid in whole well-width range from thin-well to wide-well limits. Based on this theory, we did a set of numerical calculations. General properties and some interesting features of the exciton-phonon system and also the relative importance of every phonon mode on the exciton state were discussed and concluded in the paper.

In the present paper we extend our theory to finite polar QW's and present a theoretical method for calculating the exciton binding energies of ground state and excited states. Effects of the finite-potential barrier, exciton-optical phonon interaction, and image charge are included in our theory. An expression of the exciton binding energy with only one variational parameter is obtained. Two typical QW structures that have been extensively investigated, GaAs/Ga_{1-x}Al_xAs made of III-V compounds and Zn_{1-x}Cd_xSe/ZnSe made of II-VI compounds, are put into numerical calculations. Based on the present theory and the numerical results, we discuss the properties of the excitons in polar QW's. A more accurate calculation by including the valence-band complexity will make the study run into new complications and is not considered in the present paper.

We describe the theory in Sec. II and present numerical results in Sec. III. Discussions and comparisons with experiments are included in Sec. III. The conclusions are given in Sec. IV.

II. THEORY

Within the framework of effective-mass and nondegenerate-band approximations, the Hamiltonian of an exciton interacting with optical phonons in a finite QW composed of two polar compounds is expressed in three parts as

$$H = H_e + H_{\text{ph}} + H_i. \quad (2.1)$$

The free-exciton Hamiltonian is written as

$$H_e = \sum_j \left\{ \frac{P_{j\parallel}^2}{2m_{j\parallel}} + \frac{P_{jz}^2}{2m_{jz}} + V(z_j) \right\} + V_{e-h}(\rho, z_e, z_h), \quad (2.2)$$

with

$$m_{j\nu} = \begin{cases} m_{j\nu w}, & |z_j| \leq d \\ m_{j\nu b}, & |z_j| > d \end{cases} \quad (j=e, h; \nu=\parallel, z) \quad (2.3)$$

and

$$V(z_j) = \begin{cases} 0, & |z_j| \leq d \\ v_j, & |z_j| > d \end{cases} \quad (j=e, h), \quad (2.4)$$

where $j=e, h$ refers to the electron and hole, respectively. $\mathbf{P}_j = (\mathbf{P}_{j\parallel}, P_{jz})$, $\mathbf{r}_j = (\boldsymbol{\rho}_j, z_j)$ and $m = (m_{j\parallel}, m_{jz})$ are the momentum, position, and effective band mass of the particles. $\mathbf{P}_{j\parallel}$ and $\boldsymbol{\rho}_j$ are two-dimensional vectors in the x - y plane. $V(z_j)$ for $j=e$ ($j=h$) is the barrier potential experienced by the electron (hole). The width of the QW is $W (=2d)$.

$V_{e-h}(\rho, z_e, z_h)$ is the electron-hole Coulomb interaction potential in the QW system. Its expression can be evaluated by the image charge method and has been studied in detail by Kumagai and Takagahara.¹² The expression can be given in the form of infinite series and is very lengthy in the case of a finite QW. When both the electron and the hole are in the well, for example, the electron-hole potential $V_{e-h}(\rho, z_e, z_h)$ is given by

$$V_{e-h}(\rho, z_e, z_h) = - \sum_{n=-\infty}^{\infty} \frac{\xi^{|n|} e^2}{\epsilon_{\infty 1} \sqrt{\rho^2 + [z_e - (-1)^n z_h + nW]^2}}, \quad (2.5)$$

with

$$\xi = \frac{\epsilon_{\infty 1} - \epsilon_{\infty 2}}{\epsilon_{\infty 1} + \epsilon_{\infty 2}}, \quad (2.6)$$

where the subscript $i=1$ and 2 refers to the well and the barrier, respectively. ϵ_{0i} ($\epsilon_{\infty i}$) is the static (optical) dielectric constant of the material indicated by i . Here we do not write the full expression of the potential again, and refer to Ref. 12. It has been pointed out that the self-polarization energy of the electron (hole) can be satisfactorily accounted for by a shift in the subband energy, without significant modification of the subband wave functions.¹²⁻¹⁴ Since such shifts are canceled out in the results of the exciton binding energies, the self-polarization energy will be not included in this work.

The free-phonon Hamiltonian H_{ph} is given by

$$H_{\text{ph}} = \sum_{\beta} \sum_{\mathbf{k}} \hbar \omega_{\beta}(\mathbf{k}) a_{\mathbf{k}\beta}^{\dagger} a_{\mathbf{k}\beta}, \quad (2.7)$$

where $a_{\mathbf{k}\beta}^{\dagger}$ ($a_{\mathbf{k}\beta}$) is the creation (annihilation) operator of an optical phonon with frequency $\omega_{\beta}(\mathbf{k})$ and wave vector (\mathbf{k}, k_{β}) . The two-dimensional (2D) vector \mathbf{k} denotes the wave vector in the x - y plane. $\beta=m$ refers to the confined LO phonon in the well material with frequency ω_{L1} and the wave vector along the z axis $k_m = m\pi/W$. $\beta=z$ describes the half-space LO phonon in the barrier range with frequency ω_{L2} and wave vector (\mathbf{k}, k_z) . $\beta=(\sigma, p)$ refers to the interface optical (IO) phonon. The IO phonon is the vibration in the x - y plane and $k_{\beta}=0$. The index p ($=+, -$) refers to the symmetric and antisymmetric IO phonon models, and σ ($=+, -$) to the high- and low-frequency IO phonon modes,

respectively. The dispersion relation of the frequency $\omega_{\sigma p}$ has been given in our previous paper.²⁶

The exciton-LO-phonon interaction Hamiltonian takes the form of

$$H_i = \sum_{\beta} \sum_{\mathbf{k}} \{ V_{\mathbf{k}\beta} [L_{\mathbf{k}\beta}(z_e) \exp(i\mathbf{k} \cdot \boldsymbol{\rho}_e) - L_{\mathbf{k}\beta}(z_h) \exp(i\mathbf{k} \cdot \boldsymbol{\rho}_h)] a_{\mathbf{k}\beta} + \text{H.c.} \}, \quad (2.8)$$

The coefficients $V_{\mathbf{k}\beta}$ and $L_{\mathbf{k}\beta}(z_j)$ ($j=e,h$) of the confined LO phonons take the form of

$$V_{km} = i \left[\frac{\hbar \omega_{L1}}{2dS} \left(\frac{1}{\epsilon_{\infty 1}} - \frac{1}{\epsilon_{01}} \right) \frac{4\pi e^2}{k^2 + k_m^2} \right]^{1/2}, \quad (2.9)$$

$$L_{km}(z_j) = \sin[k_m(z_j + d)] \theta(d - |z_j|) \quad (j=e,h), \quad (2.10)$$

where S stands for the area of the interface. $\theta(x)$ is a stage function with $\theta(x)=1$ when $x>0$ and $\theta(x)=0$ when $x \leq 0$. The coefficients of the half-space LO phonon take the form of

$$V_{kz} = i \left[\frac{\hbar \omega_{L2}}{DS} \left(\frac{1}{\epsilon_{\infty 2}} - \frac{1}{\epsilon_{02}} \right) \frac{4\pi e^2}{k^2 + k_z^2} \right]^{1/2}, \quad (2.11)$$

$$L_{kz}(z_j) = \sin[k_z(|z_j| - d)] \theta(|z_j| - d) \quad (j=e,h), \quad (2.12)$$

where D is the barrier width. The coefficients of IO phonons takes the form of

$$V_{k,\sigma p} = i \left(\frac{\hbar \omega_{\sigma p}}{S} \frac{1 + p e^{-2kd}}{\epsilon_{p1} \xi_{1\sigma p} + \epsilon_{p2} \xi_{2\sigma p}} \frac{\pi e^2}{k} \right)^{1/2}. \quad (2.13)$$

$$L_{k,\sigma+}(z_j) = \begin{cases} \exp[-k(z_j - d)], & z_j > d \\ \cosh(kz_j) / \cosh(kd), & -d \leq z_j \leq d \\ \exp[k(z_j + d)], & z_j < -d, \end{cases} \quad (2.14)$$

$$L_{k,\sigma-}(z_j) = \begin{cases} \exp[-k(z_j - d)], & z_j > d \\ \sinh(kz_j) / \sinh(kd), & -d \leq z_j \leq d \\ -\exp[k(z_j + d)], & z_j < -d, \end{cases} \quad (2.15)$$

with

$$\xi_{i\sigma p}(kd) = \left(\frac{\omega_{Li}^2 - \omega_{Ti}^2}{\omega_{Ti}^2 - \omega_{\sigma p}^2} \right)^2 \frac{\omega_{\sigma p}^2 \epsilon_i}{\omega_{Ti}^2 \epsilon_{0i}} \quad (i=1,2), \quad (2.16)$$

where ω_{Li} (ω_{Ti}) is the longitudinal (transverse) optical phonon frequency of the material indicated by i . The total trial wave function of the exciton-phonon system is a product of the exciton wave function and the phonon wave function, and it takes the forms of

$$|\Psi\rangle = U(f)|0\rangle |\Psi_{n,l_1,l_2}\rangle. \quad (2.17)$$

The phonon state is assumed as a coherentlike state $U(f)|0\rangle$, where $|0\rangle$ is the zero phonon state, $U(f)$ is an unitary transformation operator, which is defined as

$$U(f) = \exp \left\{ \sum_{\beta} \sum_{\mathbf{k}} \sum_j [f_{\mathbf{k}\beta j} L_{\mathbf{k}\beta}(z_j) \times \exp(-i\mathbf{k} \cdot \boldsymbol{\rho}_j) a_{\mathbf{k}\beta}^{\dagger} - \text{H.c.}] \right\}, \quad (2.18)$$

where $f_{\mathbf{k}\beta j}$ will be determined later by the variational condition.

$\Psi_{n,l_1,l_2}(\boldsymbol{\rho}, z_1, z_2)$ is assumed as a product of the exciton wave function for the relative coordinate-dependent term and subband wave functions of the electron and hole in the QW. The effects of finite confinement, subbands of the electron and hole, and the internal excited states of the exciton are included in the function. Usually the following variational wave function is used:

$$\Psi_{n,l_1,l_2}(\boldsymbol{\rho}, z_1, z_2, \lambda) = N_{n,l_1,l_2} \phi_n(\mathbf{r}, \lambda) \psi_{l_1}(z_1) \psi_{l_2}(z_2), \quad (2.19)$$

where the constant N_{n,l_1,l_2} is determined by the normalization condition. $\phi_n(\mathbf{r}, \lambda)$ is the exciton wave function of the relative motion with the quantum number n . For the $1s$ and $2s$ exciton states the wave functions are chosen as, respectively,

$$\phi_{1s}(\mathbf{r}, \lambda) = \exp(\lambda_1 r), \quad (2.20)$$

$$\phi_{2s}(\mathbf{r}, \lambda) = (1 - Ar) \exp(\lambda_2 r), \quad (2.21)$$

where λ_1 and λ_2 are variational parameters, which will be determined numerically by minimizing the energy of the system. A is determined by the orthogonalization condition. $\psi_{l_1}(z_1)$ and $\psi_{l_2}(z_2)$ are the wave functions of the electron and hole moving in the finite QW in the subband l_1 and l_2 , respectively. In the assumption of this paper $\psi_{l_1}(z_1)$ and $\psi_{l_2}(z_2)$ can be written by

$$\psi_{l_j}(z_j) = \begin{cases} \cos(k_{lj}d) e^{-k'_{lj}(|z_j| - d)}, & |z_j| > d \\ \cos(k_{lj}z_j), & |z_j| \leq d \end{cases} \quad j=e,h; \quad l=1,3,5,\dots \quad (2.22)$$

and

$$\psi_{l_j}(z_j) = \begin{cases} \text{sgn}(z_j) \sin(k_{lj}d) e^{-k'_{lj}(|z_j| - d)}, & |z_j| > d \\ \sin(k_{lj}z_j), & |z_j| \leq d \end{cases} \quad j=e,h; \quad l=2,4,6,\dots \quad (2.23)$$

where the wave numbers k_{lj} and k'_{lj} are related to the subband energy E_{lj} with

$$k_{lj} = \left(\frac{2m_{jzw} E_{lj}}{\hbar^2} \right)^{1/2}, \quad (2.24)$$

$$k'_{lj} = \left(\frac{2m_{jzb}(v_j - E_{lj})}{\hbar^2} \right)^{1/2}. \quad (2.25)$$

According to Bastard's work,²⁷ the subband wave function should satisfy the boundary conditions of $\psi_{l_j}(z_j)$ and $(\partial\psi_{l_j}/\partial z_j)/m_{jz}$, which are both continuous on the interface ($z_j = \pm d$), which gives

$$k_{l_j}\tan(k_{l_j}d) = \frac{m_{jw}}{m_{jb}}k'_{l_j}, \quad l = 1, 3, 5, \dots, \quad (2.26)$$

$$k_{l_j}\cot(k_{l_j}d) = -\frac{m_{jw}}{m_{jb}}k'_{l_j}, \quad l = 2, 4, 6, \dots \quad (2.27)$$

The subband energy E_{l_j} is determined by numerically solving the transcendental equations (2.26) and (2.27) for the finite square wells. By the same variational method as shown in Ref. 26, the energy of the exciton-optical phonon system is given by

$$\begin{aligned} E &= \langle \Psi | H | \Psi \rangle = \langle \Psi_{n,l_1,l_2} | \langle 0 | U(F) | H | U(F) | 0 \rangle | \Psi_{n,l_1,l_2} \rangle \\ &= E_0 + \sum_{\beta} \sum_{\mathbf{k}} \sum_j B_{\mathbf{k}\beta j} |f_{\mathbf{k}\beta j}|^2 + \sum_{\beta} \sum_{\mathbf{k}} \{ f_{\mathbf{k}\beta e}^* f_{\mathbf{k}\beta h} G_{\mathbf{k}\beta} \\ &\quad + f_{\mathbf{k}\beta e} f_{\mathbf{k}\beta h}^* G_{\mathbf{k}\beta}^* \} - \sum_{\beta} \sum_{\mathbf{k}} \{ Q_{\mathbf{k}\beta e} f_{\mathbf{k}\beta e}^* + Q_{\mathbf{k}\beta h} f_{\mathbf{k}\beta h}^* \\ &\quad + Q_{\mathbf{k}\beta e}^* f_{\mathbf{k}\beta e} + Q_{\mathbf{k}\beta h}^* f_{\mathbf{k}\beta h} \}. \end{aligned} \quad (2.28)$$

with the following abbreviations:

$$\begin{aligned} E_0 &= \left\langle \Psi_{n,l_1,l_2} \left| \frac{p^2}{2m_{\parallel}} + V_{e-h}(\rho, z_e, z_h) \right. \right. \\ &\quad \left. \left. + \sum_j \left\{ \frac{p_{jz}^2}{2m_{jz}} + V(z_j) \right\} \right| \Psi_{n,l_1,l_2} \right\rangle, \end{aligned} \quad (2.29)$$

$$A_{\mathbf{k}\beta j} = \langle \Psi_{n,l_1,l_2} | L_{\mathbf{k}\beta}^2(z_j) | \Psi_{n,l_1,l_2} \rangle, \quad (2.30)$$

$$\begin{aligned} B_{\mathbf{k}\beta j} &= \left\langle \Psi_{n,l_1,l_2} \left| \left\{ \hbar \omega_{\beta}(\mathbf{k}) + \frac{\hbar^2 k^2}{2m_{j\parallel}} \right\} L_{\mathbf{k}\beta}^2(z_j) \right. \right. \\ &\quad \left. \left. + \frac{\hbar^2}{2m_{jz}} \left(\frac{\partial L_{\mathbf{k}\beta}(z_j)}{\partial z_j} \right)^2 \right| \Psi_{n,l_1,l_2} \right\rangle, \end{aligned} \quad (2.31)$$

$$C_{\mathbf{k}\beta} = \langle \Psi_{n,l_1,l_2} | L_{\mathbf{k}\beta}(z_1) L_{\mathbf{k}\beta}(z_2) \exp(i\mathbf{k} \cdot \boldsymbol{\rho}) | \Psi_{n,l_1,l_2} \rangle, \quad (2.32)$$

$$G_{\mathbf{k}\beta} = \hbar \omega_{\beta}(\mathbf{k}) C_{\mathbf{k}\beta}, \quad (2.33)$$

$$Q_{\mathbf{k}\beta e} = -V_{\mathbf{k}\beta}^* (A_{\mathbf{k}\beta e} - C_{\mathbf{k}\beta}), \quad Q_{\mathbf{k}\beta h} = V_{\mathbf{k}\beta}^* (A_{\mathbf{k}\beta h} - C_{\mathbf{k}\beta}^*), \quad (2.34)$$

where E_0 is the bare-exciton energy, i.e., the energy of an exciton in the QW without exciton-phonon interaction. The parameter $f_{\mathbf{k}\beta j}$ has been determined by the variational condition $\delta \langle \Psi | H | \Psi \rangle / \delta f_{\mathbf{k}\beta j} = 0$, which yields²⁶

$$f_{\mathbf{k}\beta e} = \frac{Q_{\mathbf{k}\beta e} B_{\mathbf{k}\beta h} - Q_{\mathbf{k}\beta h} G_{\mathbf{k}\beta}}{B_{\mathbf{k}\beta e} B_{\mathbf{k}\beta h} - |G_{\mathbf{k}\beta}|^2}, \quad (2.35)$$

$$f_{\mathbf{k}\beta h} = \frac{Q_{\mathbf{k}\beta h} B_{\mathbf{k}\beta e} - Q_{\mathbf{k}\beta e} G_{\mathbf{k}\beta}^*}{B_{\mathbf{k}\beta e} B_{\mathbf{k}\beta h} - |G_{\mathbf{k}\beta}|^2}.$$

Insert Eq. (2.35) into Eq. (2.28), and the general expression of the bound-state energy of the exciton-phonon interaction system is given in a very abbreviated form:

$$E = E_0 - \sum_{\beta} \sum_{\mathbf{k}} \frac{B_{\mathbf{k}\beta e} |Q_{\mathbf{k}\beta h}|^2 + B_{\mathbf{k}\beta h} |Q_{\mathbf{k}\beta e}|^2 - Q_{\mathbf{k}\beta e} Q_{\mathbf{k}\beta h}^* G_{\mathbf{k}\beta}^* - Q_{\mathbf{k}\beta e}^* Q_{\mathbf{k}\beta h} G_{\mathbf{k}\beta}}{B_{\mathbf{k}\beta e} B_{\mathbf{k}\beta h} - |G_{\mathbf{k}\beta}|^2}. \quad (2.36)$$

In Eq. (2.36) only one variation parameter (λ_1 or λ_2) that is related to the practical QW structure is needed to be determined by the numerical variation method. The second term in Eq. (2.36) is just the contribution of the exciton-LO-phonons interaction. As the same analysis as in our previous paper,²⁶ it is proved that we can use Eq. (2.36) to calculate the 1s and 2s exciton binding energies and the exciton-LO-phonon interaction energy and also the contributions of ev-ery phonon mode in finite polar QW's.

III. RESULTS AND DISCUSSIONS

Two extensively studied QW structures, GaAs/Ga_{1-x}Al_xAs and Zn_{1-x}Cd_xSe/ZnSe, are put into numerical calculations to show quantitative properties of excitons in polar QW's. In order to compare the present results with other theoretical works and experimental data, we use the isotropic effective-mass approximation in the calculation. The calculation including the anisotropic effect of the va-

lence band will be shown later in this section. For lack of physical parameters of ternary mixed crystals, the ternary material parameter $P_{A_{1-x}B_xC}$ can be derived from binary parameters P_{AC} and P_{BC} by linear interpolation relation:

$$P_{A_{1-x}B_xC} = (1-x)P_{AC} + xP_{BC}.$$

The linear interpolation scheme is a useful tool for estimating some physical parameters of alloy compounds. The physical parameters of the binary materials studied here are listed in Table I.

First, a calculation of the GaAs/Ga_{1-x}Al_xAs system as a typical example of III-V systems is presented. Since the optical phonons in Ga_{1-x}Al_xAs exhibit a two-mode behavior, it is a usual way to use the effective phonon approximation. The effective phonon energies are given by²⁸

$$\hbar \omega_L = 36.25 + 1.83x + 17.12x^2 - 5.11x^3 \quad (\text{meV}),$$

TABLE I. Physical parameters of some binary materials. Here m_0 is the mass of a free electron, a is the lattice constant, and E_g is the energy band gap.

	ϵ_0	ϵ_∞	$\hbar\omega_L$ (meV)	$\hbar\omega_T$ (meV)	m_e (m_0)	m_h (m_0)	a (\AA)	E_g (eV)
GaAs ^a	13.18	10.89	36.25	33.29	0.067	0.62	5.6533	1.424
AlAs ^a	10.06	8.16	50.09	44.88	0.150	0.76	5.6611	2.168
CdSe ^b	10.16	6.2	25.93	20.47	0.11	0.44	6.052	1.9
ZnSe ^b	7.6	5.4	31.39	26.43	0.13	0.57	5.668	2.82

^aReference 28.

^bReference 35.

$$\hbar\omega_T = 33.29 + 10.70x + 0.03x^2 + 0.86x^3 \quad (\text{meV}).$$

The energy band-gap discontinuity at the interface is given by $\Delta E_g = 1.155x + 0.37x^2$ (eV).²⁸ The potential-well heights v_e and v_h are assumed to be 60% and 40% of ΔE_g ,²⁹ respectively.

As shown in Fig. 1 the $1s$ and $2s$ exciton binding energies of GaAs/Ga_{1-x}Al_xAs QW's increase with increasing the aluminum concentrations x in the barrier. The quantum confinement effect is significant for the $1s$ exciton but much less significant for the $2s$ exciton with its smaller binding energy. This fact can be explained qualitatively based on the simple infinite QW theory.² As well known, the exciton energy levels are given by R_y/n^2 in the 3D limit and $R_y/(n - \frac{1}{2})^2$ in the 2D limit, where R_y [$=\mu_1 e^4/2\hbar^2 \epsilon_\infty^2$] is the Rydberg energy and $n=1,2,\dots$. When the well width is changed from infinite to zero the $1s$ exciton binding energy varies from R_y to $4R_y$, i.e., $E_{1s}^{2D}/E_{1s}^{3D}=4$. However, at the same time, the $2s$ exciton binding energy only varies from $R_y/4$ to $4R_y/9$, i.e., $E_{2s}^{2D}/E_{2s}^{3D}=16/9$, which is much smaller than that of the $1s$ exciton. In the finite-well case we believe that E_{2s}^{2D}/E_{2s}^{3D} will be smaller than $16/9$ and closer to 1. The $2s$ exciton binding energy is a smooth function of the well width W and the barrier-potential height, which is proportional to the alloy concentration x . By analyzing the calculated data, we obtain a simple equation for estimating the $2s$ exciton binding energy E_{2s}^b in the GaAs/Ga_{1-x}Al_xAs QW:

$$E_{2s}^b \quad (\text{meV}) = 1.7 + 1.4x - (1.2 + 3.6x)10^{-3} W(\text{\AA})$$

$$(30 \leq W \leq 300 \text{\AA} \text{ and } 0.4 \geq x \geq 0.05).$$

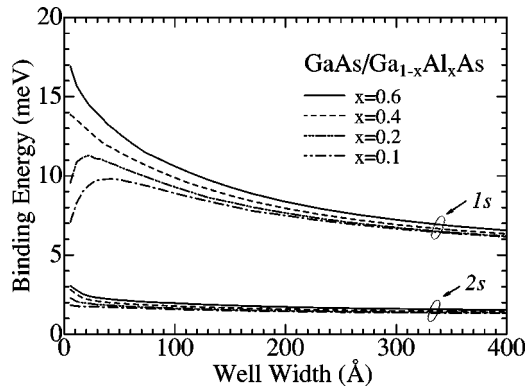


FIG. 1. Binding energies of the $1s$ and $2s$ excitons in GaAs/Ga_{1-x}Al_xAs quantum wells as functions of the well width.

The most reliable experiment of the exciton binding energy is the photoluminescence experiment on the high-quality QW sample, where two clearly resolved peaks are identified as $1s$ and $2s$ exciton states. The value of $|E_{2s} - E_{1s}|$ is directly measured from the distance of the two peaks. The first observation of the discrete peaks in the low-temperature photoluminescence spectra of GaAs/Ga_{1-x}Al_xAs QW's was made by Dawson *et al.*³⁰ Two years later, well-resolved higher excited states of excitons in 225- \AA GaAs/Ga_{1-x}Al_xAs QW's were observed by Reynolds *et al.*³¹ It is believed that these experiments are accurate and reliable. Since the present theory can calculate the energy difference of the $1s$ and $2s$ excitons, it is possible to compare our theoretical results directly with the experiment data. Our theoretical results and some published experimental data are plotted in Fig. 2 with lines and points, respectively. If the uncertainty, about ± 0.35 meV,³² of the experimental data caused by the uncertainty of the ± 1 monolayer in the well width is well understood, then it is considered that the agreement of our theory with the experiments is very good in wide-well ranges.

In Fig. 3 we plot the $1s$ and $2s$ exciton-optical-phonons interaction energy in a GaAs/Ga_{0.6}Al_{0.4}As QW as a function of the well width. In order to see the relative importance of every phonon mode, the contributions of the confined LO phonon, the half-space LO phonon, and the IO phonons are also plotted in the figure, respectively. It is shown that the contribution of the half-space LO phonon is reduced very quickly to zero with the well-width increase. When the well-width is larger than 50 \AA , the half-space LO phonon is really

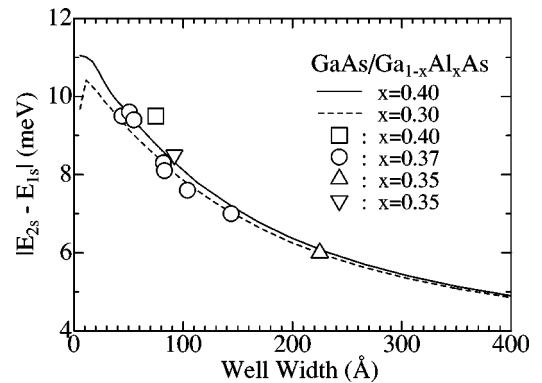


FIG. 2. Comparison of theoretical and experimental values of the energies difference between the $1s$ and $2s$ exciton states in GaAs/Ga_{1-x}Al_xAs quantum wells. The experimental points correspond to \square , Ref. 30 ($x=0.40$); \circ , Ref. 1 ($x=0.37$); \triangle , Ref. 31 ($x=0.35$); ∇ , Ref. 30 ($x=0.35$).

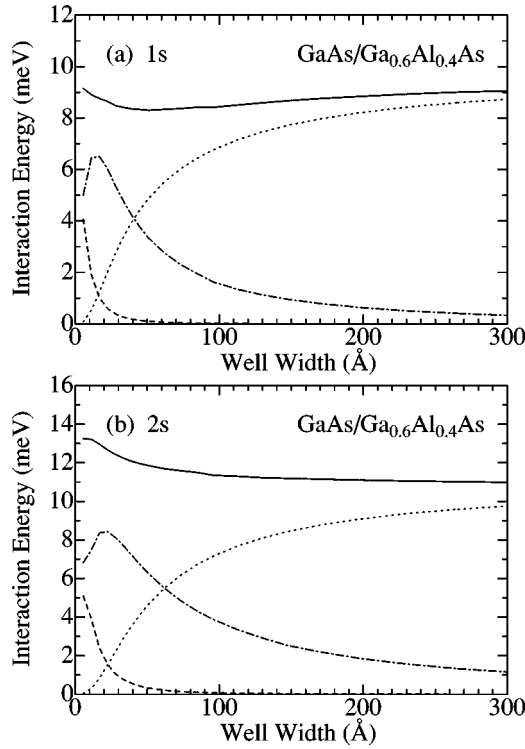


FIG. 3. $1s$ (a) and $2s$ (b) exciton–optical-phonon interaction energies in GaAs/Ga_{0.6}Al_{0.4}As quantum wells as functions of the well width. The solid line is the interaction energy of the exciton with all optical phonons, the dotted, dashed, and dash-dotted lines are the contributions of the confined LO phonon, the half-space LO phonon, and the IO phonons, respectively.

no interaction with the excitons. Comparing Figs. 3(a) and 3(b), we found that the total $2s$ exciton–optical-phonons interaction energy increases monotonously with decreasing the well width, and is always larger than that of the $1s$ exciton. The larger exciton–optical-phonon interaction of the excited state arises from the smaller cancellation of the polaron effects of the electron and the hole due to the larger exciton radii as in the case of bulk crystals.^{33,34}

By analyzing the calculated data in detail we find that the inclusion of the image charge potential increases obviously the $1s$ exciton binding energy in a GaAs/Ga_{1-x}Al_xAs QW with $x > 0.2$. This fact improves the agreement of the theory with the experiment in the cases of the well width larger than 50 Å.

Next we pay attention to the Zn_{1-x}Cd_xSe/ZnSe QW system as a typical example of II-VI systems. As pointed out by Cingolani *et al.*,²³ most of the required parameters are not very well known for ZnSe, CdSe, and their ternary alloys. Theoretical and experimental studies used rather different values of the parameters. In the present calculation we use the parameters³⁵ that are used by many other authors. The parameters of Zn_{1-x}Cd_xSe are evaluated by linear interpolation from the ZnSe and CdSe parameters. Since there is a strain effect, the conduction- and heavy-hole-valence-band offsets v_e and v_h of the Zn_{1-x}Cd_xSe/ZnSe QW are complex functions of the well width and the Cd concentration x . In this work we do not discuss the details and use a simple linear relation of $\Delta E_g = 920x$ (meV). This approximation has little effect on the quantitative properties, but has no

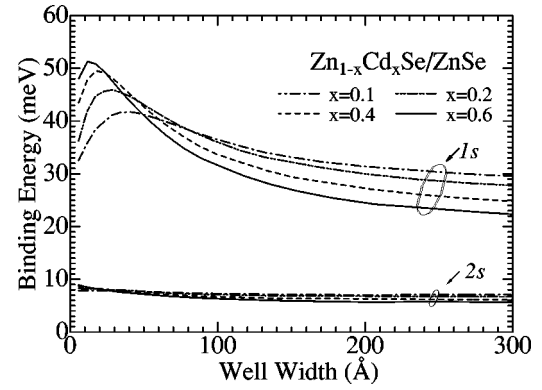


FIG. 4. Binding energies of the $1s$ and $2s$ excitons in Zn_{1-x}Cd_xSe/ZnSe quantum wells as functions of the well width.

obvious effect on the qualitative properties studied in the present paper. v_e and v_h are assumed to be 80% and 20% of ΔE_g ,²³ respectively.

The calculated exciton binding energies of Zn_{1-x}Cd_xSe/ZnSe QW's are plotted in Fig. 4. Very different from the situation of GaAs/Ga_{1-x}Al_xAs QW's, the relationship of the binding energy with the Cd concentration in the wide-well case is qualitatively different from that in the narrow-well case. When the width is larger than about 90 Å the $1s$ exciton binding energy is decreased by increasing the concentration x , but in the very narrow-well case the situation is the opposite. This interesting phenomenon also occurs for the $2s$ exciton. The $2s$ exciton binding energy of the Zn_{1-x}Cd_xSe/ZnSe QW's shows a smooth and small change in the wells. Based on the calculation a useful equation to estimate the $2s$ exciton binding energy E_{2s}^b of Zn_{1-x}Cd_xSe/ZnSe QW's is given by

$$E_{2s}^b \text{ (meV)} = 7.9 + 0.16x - (3.1 + 14.0x)10^{-3} W(\text{Å})$$

$$(30 \leq W \leq 300 \text{ Å and } x \geq 0.05).$$

The comparison of the theoretical results of $|E_{2s} - E_{1s}|$ in Zn_{1-x}Cd_xSe/ZnSe QW's with the experimental data is shown in Fig. 5. The experimental data of $|E_{2s} - E_{1s}|$ of Zn_{1-x}Cd_xSe/ZnSe QW's has rarely been published since the difficulty of making the high-quality QW structure. The only

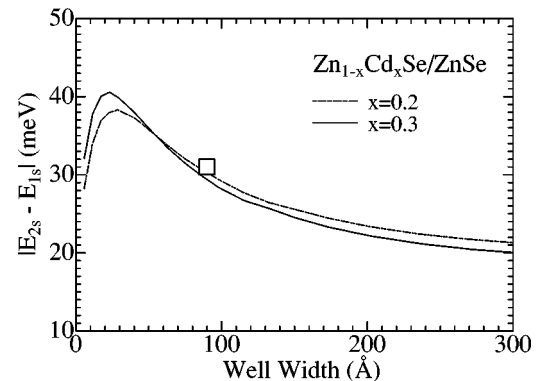


FIG. 5. Comparison of theoretical and experimental values of the energy difference between the $1s$ and $2s$ exciton states in Zn_{1-x}Cd_xSe/ZnSe quantum wells. The experimental point \square is taken from Ref. 22 ($x = 0.25 - 0.3$).

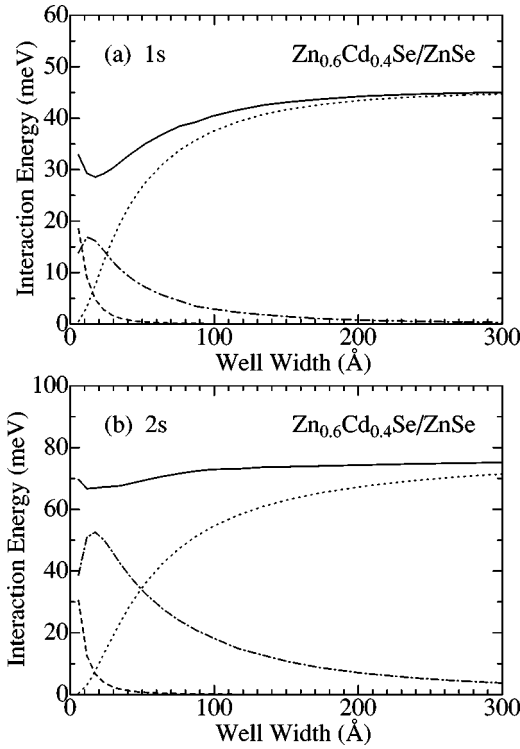


FIG. 6. $1s$ (a) and $2s$ (b) exciton–optical-phonon interaction energies in $\text{Zn}_{0.6}\text{Cd}_{0.4}\text{Se}/\text{ZnSe}$ quantum wells as functions of the well width. The solid line is the interaction energy of the exciton with all optical phonons, the dotted, dashed, and dash-dotted lines are the contributions of the confined LO phonon, the half-space LO phonon, and the IO phonons, respectively.

data are taken from Ref. 22 with the alloy concentration $x = 0.25\text{--}0.3$. It is shown that the theoretical result is in agreement with the experiment. The calculated binding energy of the quasi-2D exciton in the $\text{Zn}_{0.7}\text{Cd}_{0.3}\text{Se}/\text{ZnSe}$ QW with well thickness $W=90$ Å is about 38 meV, a value that is larger than the LO phonon energy of the well material.

The $1s$ and $2s$ exciton–phonon-interaction energies in $\text{Zn}_{0.6}\text{Cd}_{0.4}\text{Se}/\text{ZnSe}$ QW's are plotted in Figs. 6(a) and 6(b) with solid lines, respectively. The contributions from the confined LO phonon, the half-space LO phonon, and the IO phonon are plotted separately in the figure. Since the dielectric constant of the barrier is close to that of the well, the IO phonon oscillation strength is relatively small and the contribution of the IO phonon is also relatively small. The contribution of the image potential is also small because of the same reason. Comparing Figs. 3 and 6, we see that the exciton–phonon-interaction energy in II-VI QW's is much larger than that in III-V QW's.

It is seen from the figures that all of our theoretical results have features expected physically in the entire well-width range: for very wide QW's all the results are close to the corresponding 3D values of the well material and the contribution of the confined LO phonon is important; for very narrow QW's the results are close to the 3D values of the barrier material and the half-space LO phonon becomes important; in the intermediate region the quasi-2D behavior of the exciton is described correctly.

It is well known that the exciton Rydberg energy R_y and the exciton Bohr radius $a_B (= \hbar^2 \epsilon_{\infty 1} / \mu_1 e^2)$ are characteristic

parameters for analyzing the quantum-size effect of the exciton binding energy. In the case of a simple infinite-barrier QW model,² whether III-V or II-VI QW's, $E_{1s}^b/R_y \rightarrow 1$ when $W/a_B \rightarrow$ large; E_{1s}^b/R_y increases monotonously with decreasing W/a_B , and $E_{1s}^b/R_y \rightarrow 4$ when $W/a_B \rightarrow 0$. If the exciton-phonon interaction and the image potential are also included in the problem, as studied in detail in our previous paper,²⁶ the dependence of E^b/R_y upon W/a_B becomes complex. In the present paper the finite-barrier effect is also considered together with other effects, so that the dependence becomes much complex. As shown in Figs. 1 and 4, if the QW is very narrow or the barrier height is very low because of the small alloy concentration x , the exciton wave function penetrates into the finite barrier, obviously, and then the value of E_{1s}^b/R_y will become a more complex function of physical parameters of the QW structure. In these cases E_{1s}^b/R_y cannot be estimated simply based on the simple model. On the other hand, in the case of the larger concentration where the barrier height is larger and the penetration effect is very small, the quantum size dependence has no essential change from the simple infinite-barrier model. For example, it can be found from Figs. 1 and 4 that when $W/a_B=1$, $E_{1s}^b/R_y = 2.02$ for $\text{GaAs}/\text{Ga}_{0.6}\text{Al}_{0.4}\text{As}$ QW ($a_B=110$ Å and $R_y=4.7$ meV), and $E_{1s}^b/R_y=2.48$ for $\text{Zn}_{0.6}\text{Cd}_{0.4}\text{Se}/\text{ZnSe}$ QW ($a_B=42$ Å and $R_y=18.1$ meV), where a_B and R_y are calculated based on the data of Table I. These values of E_{1s}^b/R_y are very close to 2.17, the value of E_{1s}^b/R_y of the simple infinite-barrier QW model² in the same $W/a_B=1$ case.

Next we pay attention to the well thickness corresponding to the maximal exciton binding energy, which is by no way obvious for $\text{GaAs}/\text{Ga}_{1-x}\text{Al}_x\text{As}$ and $\text{Zn}_{1-x}\text{Cd}_x\text{Se}/\text{ZnSe}$ QW's, although the exciton Bohr radii are very different. As had been analyzed in our previous paper,²⁶ the quantum confinement effect and the image potential (when $\epsilon_{1\infty} > \epsilon_{2\infty}$) will increase the exciton binding energy as the well width is reduced. In the infinite QW case, these two effects will make the binding energy increase monotonously to the largest value at the 2D limit. In the opposite case, the penetration effect of the exciton to the barrier region in a finite QW will decrease the binding energy in thinner well cases.^{4,32} The competition of the three effects makes the characters of the excitons in thinner well cases, so that, if there is a maximum of the binding energy, it is caused essentially by the penetration effect. The exciton Bohr radius has no direct effect to the width corresponding to the maximal binding energy. In reality, for both of the QW structures studied here, the smaller the alloy concentration x the lower the potential barrier, so that the stronger the penetration effect, the larger the well thickness corresponding to the maximal exciton binding energy. This is clearly seen in Figs. 1 and 4.

The ratio of the LO phonon energy $\hbar\omega_{L1}$ to the exciton Rydberg energy R_y is often used to estimate qualitative properties of exciton-LO phonon interaction systems. As discussed by many authors,³⁶ the effective dielectric constant ϵ_{eff} for the LO-phonon mediated screening of the e - h interaction in an exciton is given by ϵ_0 or ϵ_{∞} according to $R_y \ll \hbar\omega_{1L}$ or $R_y \gg \hbar\omega_{1L}$. It is believed that the polaronic effect is very large in the former case and is small in the latter case. GaAs is a III-V material with very small exciton Rydberg

TABLE II. The data of γ_1 and γ_2 are from Ref. 7. The heavy-hole masses of GaAs and AlAs are calculated from γ_1 and γ_2 . The masses of $\text{Ga}_{1-x}\text{Al}_x\text{As}$ are obtained by the linear interpolation relation from the masses of GaAs and AlAs. The masses are in the unit of the free-electron mass.

	γ_1	γ_2	$m_{h\parallel}$	m_{hz}
GaAs	6.85	2.1	0.112	0.377
AlAs	3.45	0.68	0.242	0.478
$\text{Ga}_{1-x}\text{Al}_x\text{As}$			$0.112+0.130x$	$0.377+0.101x$

energy $R_y \approx 4.7$ meV,²⁸ which is much smaller than the LO phonon energy $\hbar\omega_{1L} \approx 36$ meV. So that the exciton-LO-phonon interaction modifies greatly the property of the exciton and has to be taken into consideration, in spite of the very small electron-LO-phonon coupling constant α_e [≈ 0.068 (Ref. 28)]. The effective dielectric constant ϵ_{eff} for the screening of the Coulomb interaction in GaAs is approximately ϵ_0 and the exciton binding energy is very close to the hydrogenic exciton binding energy with the static dielectric constant ϵ_0 . The situation of the $\text{Zn}_{1-x}\text{Cd}_x\text{Se}/\text{ZnSe}$ QW is somewhat different. ZnSe is a II-VI material with $R_y \approx 17$ meV (Ref. 22) and $\alpha_e \approx 0.432$.³⁷ Since $R_y \sim \hbar\omega_{1L}$, the LO phonon mediated e - h interaction is complicated and the ϵ_{eff} is given by a value between ϵ_0 and ϵ_∞ . The exciton-LO-phonon interaction in ZnSe is much stronger than that in III-V materials and must be taken into account. Here it is found that although the ratios of $\hbar\omega_{1L}/R_y$ of the III-V and II-VI materials are very different, the polaronic effect is important in both cases. If one uses $\hbar\omega_{1L}/R_y$ as the only criterion of the importance of the polaronic effect, it would cause puzzlement in the understanding of the exciton-LO-phonon interaction. It is important to consider both the ratio $\hbar\omega_{1L}/R_y$ and the strength of electron (hole) -phonon coupling as the criterion. In the connection the ratio of the exciton-phonon interaction energy E_{ex-ph} to the exciton Rydberg energy R_y reflects the importance of the polaronic effect. If $E_{ex-ph} \geq R_y$, the influence of the polarons should be taken into account. Since exciton-optical interaction phonon energies shown in Figs. 3 and 6 are larger than the corresponding exciton Rydberg energies of the two QW structures, we can say that the polaronic effect is important in both of the cases, in spite of the very different ratio of $\hbar\omega_{1L}/R_y$.

In the last part of this section we discuss the anisotropic mass effects. As shown in Eqs. (2.31)–(2.36), our theory can study the problems taking into account the anisotropic mass effects in principle. A numerical calculation for the $\text{GaAs}/\text{Ga}_{1-x}\text{Al}_x\text{As}$ QW is done as an example. The heavy-hole mass can be expressed in terms of the well-known Kohn-Luttinger band parameter as⁴

$$m_{h\parallel} = m_0(\gamma_1 + \gamma_2)^{-1},$$

$$m_{hz} = m_0(\gamma_1 - 2\gamma_2)^{-1},$$

where m_0 is the free-electron mass. The parameter γ_1 , γ_2 , and the corresponding masses used in our calculation are listed in Table II. The other physical parameters used in this calculation are the same as in Table I. We notice that both

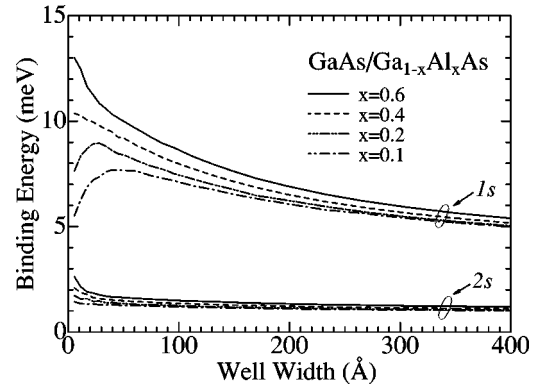


FIG. 7. Binding energies of the 1s and 2s excitons in $\text{GaAs}/\text{Ga}_{1-x}\text{Al}_x\text{As}$ quantum wells as functions of the well width calculated by taking into account the anisotropic hole-mass effect.

$m_{h\parallel}$ and m_{hz} listed in Table II are much smaller than the isotropic masses listed in Table I. Based on the analysis of Ref. 26, it is predicted that the exciton binding energy and the exciton-LO-phonon interaction energy calculated with these anisotropic masses will be smaller than the previous results. Since there is no reliable data, the further calculation is not done for the $\text{Zn}_{1-x}\text{Cd}_x\text{Se}/\text{ZnSe}$ QW.

It is seen that Fig. 7 is qualitatively the same as Fig. 1, but the value is smaller than that in Fig. 1, obviously. The value of $|E_{2s} - E_{1s}|$ calculated from Fig. 7 is smaller than the experiment value by about 1.5–2 meV. The similar smaller binding energy has also been found by Greene, Bajaj, and Phelps,⁴ who calculated the exciton binding energy in a finite QW with the Kohn-Luttinger band parameters γ_1 and γ_2 , similar to the present work, but without the detailed polaronic effect. Although the consideration of the anisotropic effects makes the calculation more complicated, the result is worse than the previous result with isotropic approximation. It is believed that the reason is simply the approximation omitting the off-diagonal terms of the Kohn-Luttinger Hamiltonian.³⁸ Based on the study of Ekenberg and Altarelli,⁷ the off-diagonal elements also give important correction to the exciton binding energies. Then we think that the presently used isotropic masses may be considered to be the masses that have taken into account effectively the valence-band complexity to some extent. It is true that an accurate method is to solve the problem by using the full Kohn-Luttinger Hamiltonian, and thus take into account properly the degeneracy of the valence band and the inter-band mixing, together with the finite confinement effect and the polaronic effect. Obviously, this is not an easy task.

IV. CONCLUSIONS

With a variational method we have presented a theoretical study on the property of excitons in polar QW's with finite potential barriers. By taking into account the effects of exciton-optical-phonon interaction, image charge potential, and discontinuity of the band masses on the interface, the expressions of the exciton binding energy and the exciton-LO phonon-interaction energy in a polar QW are presented. Our theory gives valid results throughout the entire well-width range. In the limits of thin and thick well cases the three-dimensional behavior can be obtained, and in

the intermediate region of the well width the quasi-two-dimensional behavior of the exciton is described correctly. Two typical QW structures are put into numerical calculation, and the results are discussed and compared with the experiments. It is found that our theoretical results are in good agreement with the experiment. Based on the present theory, we find the following. (A) Very different from the $1s$ exciton, the variation of $2s$ exciton binding energy with the well width and the compound concentration is smooth and small. It can be treated as a linear relation with the width and the concentration x with good accuracy. (B) The exciton-LO-phonon interaction energies of II-VI polar QW's are much larger than that of III-V polar QW's, but the ratios of the interaction energy to the exciton Rydberg energy are not very different from each other. The polaronic effect is im-

portant in both cases. (C) The consideration of the image-charge effect affects the binding energy considerably for GaAs/Ga $_{1-x}$ Al $_x$ As QW's ($x > 0.2$), but only has a little correction for Zn $_{1-x}$ Cd $_x$ Se/ZnSe QW's since the difference of $\epsilon_{\infty 1}$ and $\epsilon_{\infty 2}$ is small. (D) The $1s$ exciton-phonon interaction energies of both III-V and II-VI polar QW's are slowly reduced with the decrease of the well width until a minimum value, and then increase in the very narrow well limit.

ACKNOWLEDGMENTS

R.Z. acknowledges support from the Fund for Excellent Young University Teachers of the State Education Commission of China.

- ¹R. C. Miller, D. A. Kleinman, W. T. Tsang, and A. C. Gossard, Phys. Rev. B **24**, 1134 (1981).
- ²G. Bastard, E. E. Mendez, L. L. Chang, and L. Esaki, Phys. Rev. B **26**, 1974 (1982).
- ³M. Matsuura and Y. Shinozuka, J. Phys. Soc. Jpn. **53**, 3138 (1984).
- ⁴R. L. Greene, K. K. Bajaj, and D. E. Phelps, Phys. Rev. B **29**, 1807 (1984).
- ⁵R. L. Greene and K. K. Bajaj, Phys. Rev. B **31**, 6498 (1985).
- ⁶C. Priester, G. Allan, and M. Lannoo, Phys. Rev. B **30**, 7302 (1984).
- ⁷U. Ekenberg and M. Altarelli, Phys. Rev. B **35**, 7585 (1987).
- ⁸G. E. W. Bauer and T. Ando, Phys. Rev. B **38**, 6015 (1988).
- ⁹J. W. Wu, Phys. Rev. B **39**, 12 944 (1987).
- ¹⁰L. C. Andreani and A. Pasquarello, Phys. Rev. B **42**, 8928 (1990).
- ¹¹R. P. Leavitt and J. W. Little, Phys. Rev. B **42**, 11 774 (1990).
- ¹²M. Kumagai and T. Takagahara, Phys. Rev. B **40**, 12 359 (1989).
- ¹³D. B. Tran Thoai, R. Zimmermann, M. Grundmann, and D. Bimberg, Phys. Rev. B **42**, 5906 (1990).
- ¹⁴J. Cen, R. Chen, and K. K. Bajaj, Phys. Rev. B **50**, 10 947 (1994), and references therein.
- ¹⁵D. S. Chun, W. L. Won, and J. H. Pei, Phys. Rev. B **49**, 14 554 (1994).
- ¹⁶S. Moukhliss, M. Fliyou, and S. Sayouri, Phys. Status Solidi B **196**, 121 (1996).
- ¹⁷L. Wendler and R. Pechstedt, Phys. Status Solidi B **141**, 129 (1987).
- ¹⁸N. Mori and T. Ando, Phys. Rev. B **40**, 6175 (1989).
- ¹⁹H. J. Xie and C. Y. Chen, J. Phys.: Condens. Matter **6**, 1007 (1994).
- ²⁰B. A. Vojak, N. Holonyak, Jr., D. W. Laidig, K. Hess, J. J. Coleman, and P. D. Dapkus, Solid State Commun. **35**, 477 (1980).
- ²¹J. C. Maan, G. Belle, A. Fasolino, M. Altarelli, and K. Ploog, Phys. Rev. B **30**, 2253 (1984).
- ²²N. T. Pelekanos, J. Ding, M. Hagerott, A. V. Nurmikko, H. Luo, N. Samarth, and J. K. Furdyna, Phys. Rev. B **45**, 6037 (1992).
- ²³R. Cingolani, M. Di Dio, M. Lomascolo, R. Rinaldi, P. Prete, L. Vasanelli, L. Vanzetti, F. Bassani, A. Bonanni, L. Sorba, and A. Franciosi, Phys. Rev. B **50**, 12 179 (1995).
- ²⁴R. Cingolani, P. Prete, D. Greco, P. V. Giugno, M. Lomascolo, R. Rinaldi, L. Calcagnile, L. Vanzetti, L. Sorba, and A. Franciosi, Phys. Rev. B **51**, 5176 (1995).
- ²⁵R. S. Zheng and M. Matsuura, Phys. Rev. B **56**, 2058 (1997).
- ²⁶R. S. Zheng and M. Matsuura, Phys. Rev. B **57**, 1749 (1998).
- ²⁷G. Bastard, Phys. Rev. B **24**, 5693 (1981).
- ²⁸S. Adachi, J. Appl. Phys. **58**, R1 (1985).
- ²⁹R. C. Miller, D. A. Kleinman, and A. C. Gossard, Phys. Rev. B **29**, 7085 (1984).
- ³⁰P. Dawson, K. J. Moore, G. Duggan, H. I. Ralph, and T. B. Foxon, Phys. Rev. B **34**, 6007 (1986).
- ³¹D. C. Reynolds, K. K. Bajaj, C. Leak, G. Peters, W. Theis, P. W. Yu, K. Alavi, C. C. Colvard, and I. Shidlovsky, Phys. Rev. B **37**, 3117 (1988).
- ³²H. Mathieu, P. Lefebvre, and P. Christol, Phys. Rev. B **46**, 4092 (1992).
- ³³M. Matsuura and H. Büttner, Phys. Rev. B **21**, 679 (1980).
- ³⁴M. Matsuura, Phys. Rev. B **37**, 6977 (1988).
- ³⁵*Semiconductors-Basic Data*, edited by O. Madelung, Springer, 2nd revised ed. (Springer, Berlin, 1996), pp. 183 and 185.
- ³⁶M. Ueta, K. Kanzaki, K. Kobayashi, Y. Toyozawa, and E. Hanamura, in *Excitonic Processes in Solids*, edited by Peter Fulde (Springer, Berlin, 1986), p. 211.
- ³⁷E. Kartheuser, in *Polarons in Ionic Crystals and Polar Semiconductors*, edited by J. T. Devreese (North-Holland, Amsterdam, 1972), p. 717.
- ³⁸J. M. Luttinger and W. Kohn, Phys. Rev. **97**, 869 (1955); J. M. Luttinger, *ibid.* **102**, 1030 (1956).